Biochimica et Biophysica Acta 1833 (2013) 2322–2333

Contents lists available at SciVerse ScienceDirect

Biochimica et Biophysica Acta

journal homepage: www.elsevier.com/locate/bbamcr

The three α_1-adrenoceptor subtypes show different spatio-temporal mechanisms of internalization and ERK1/2 phosphorylation

M. Perez-Aso [a], V. Segura [a], F. Montó [a], D. Barettino [b], M.A. Noguera [a], G. Milligan [c], P. D'Ocon [a,*]

[a] Departament de Farmacologia, Universitat de València, Spain
[b] Instituto de Biomedicina de Valencia (CSIC), Spain
[c] Molecular Pharmacology Group, Institute of Neuroscience and Psychology, College of Medical, Veterinary and Life Sciences, University of Glasgow, Glasgow G12 8QQ, Scotland, UK

ARTICLE INFO

Article history:
Received 14 June 2012
Received in revised form 12 June 2013
Accepted 13 June 2013
Available online 21 June 2013

Keywords:
Adrenaline α_1 receptors
ERK1/2
PKC
Internalization
Constitutive activity

ABSTRACT

We analyzed the kinetic and spatial patterns characterizing activation of the MAP kinases ERK 1 and 2 (ERK1/2) by the three α_1-adrenoceptor (α_1-AR) subtypes in HEK293 cells and the contribution of two different pathways to ERK1/2 phosphorylation: protein kinase C (PKC)-dependent ERK1/2 activation and internalization-dependent ERK1/2 activation. The different pathways of phenylephrine induced ERK phosphorylation were determined by western blot, using the PKC inhibitor Ro 31-8425, the receptor internalization inhibitor concanavalin A and the siRNA targeting β-arrestin 2. Receptor internalization properties were studied using CypHer5 technology and VSV-G epitope-tagged receptors. Activation of α_{1A}- and α_{1B}-ARs by phenylephrine elicited rapid ERK1/2 phosphorylation that was directed to the nucleus and inhibited by Ro 31-8425. Concomitant with phenylephrine induced receptor internalization α_{1A}-AR, but not α_{1B}-AR, produced a maintained and PKC-independent ERK phosphorylation, which was restricted to the cytosol and inhibited by β-arrestin 2 knockdown or concanavalin A treatment. α_{1D}-AR displayed constitutive ERK phosphorylation, which was reduced by incubation with prazosin or the selective α_{1D} antagonist BMY7378. Following activation by phenylephrine, α_{1D}-AR elicited rapid, transient ERK1/2 phosphorylation that was restricted to the cytosol and not inhibited by Ro 31-8425. Internalization of the α_{1D}-AR subtype was not observed via CypHer5 technology. The three α_1-AR subtypes present different spatio-temporal patterns of receptor internalization, and only α_{1A}-AR stimulation translates to a late, sustained ERK1/2 phosphorylation that is restricted to the cytosol and dependent on β-arrestin 2 mediated internalization.

1. Introduction

The α_1-adrenoceptors (α_1-ARs) have been extensively investigated with regard to their pharmacology and structure–function relationship. In contrast, less is known about their regulatory properties, and the trafficking and protein interactions involved in these processes. They are heptahelical transmembrane proteins that belong to the G protein-coupled receptor (GPCR) superfamily. Upon agonist binding, α_1-ARs stimulate activation and dissociation of the α and βγ subunits of $G_{q/11}$ proteins [1], and promote PKC activation [2], as well as an increase of intracellular IP3 and calcium content [3,4]. Extracellular signal-regulated kinase (ERK)/mitogen-activated protein kinase (MAPK) activation promoted by the different α_1-AR subtypes has also been detected [5,6]. Termination of GPCR signaling is triggered by the phosphorylation of the agonist-occupied receptor by G-protein-coupled receptor-kinases (GRKs) and the second-messenger-dependent protein kinases PKA and PKC [5,7], promoting high affinity binding of cytoplasmatic β-arrestins to the receptor, resulting in its desensitization and endocytosis [8].

Three different α_1-AR subtypes (α_{1A}, α_{1B} and α_{1D}) have been cloned and exhibit differences in amino acid sequence and antagonist binding affinities [9,10]. Different cellular localization is also exhibited by the three subtypes: α_{1B}-AR is primarily expressed on the cell surface [11], α_{1A}-AR is detected not only on the cell surface, but also intracellularly [12]. In contrast, α_{1D}-AR appears to be localized perinuclearly and produces ERK1/2 activation in the absence of agonists [11]. This α_{1D}-AR constitutive activity has also been measured by a spontaneous increase in the resting tone [13–16] and calcium and IP3 accumulation [17,18] in rat aorta, where the main α_1-AR subtype is α_{1D}.

An increasing number of studies indicate that the α_1-AR subtypes display striking differences in their internalization properties and, although controversial, it has been suggested that while α_{1B}-AR undergoes

Abbreviations: α_1-AR, α_1 adrenoceptor; β_2-AR, β_2 adrenoceptor; $AT_{1A}R$, angiotensin receptor type 1A; Bmax, maximum number of binding sites; BSA, bovine serum albumin; ConA, concanavalin A; DMSO, dimethyl sulfoxide; EGFR, epidermal growth factor receptor; GAPDH, glyceraldehyde-3-phosphate dehydrogenase; GPCR, G-protein coupled receptor; GRK, G-protein-coupled receptor kinase; HEK, human embryonic kidney; KRH, Krebs Ringer Hepes; MAPK, mitogen-activated protein kinase; PCR, polymerase chain reaction; PBST, phosphate-buffered saline with 0.1% Tween 20; PE, phenylephrine; PKA, protein kinase A; PKC, protein kinase C; PTHR, parathyroid hormone receptor type 1; PZ, prazosin

* Corresponding author at: Universitat de València Facultad de Farmàcia, Departament de Farmacologia, Avda. Vicent Andres Estelles s/n, 46100 Burjassot, València, Spain. Tel.: +34 963544828; fax: +34 963544943.
E-mail address: doconp@uv.es (P. D'Ocon).

0167-4889/$ – see front matter © 2013 Elsevier B.V. All rights reserved.
http://dx.doi.org/10.1016/j.bbamcr.2013.06.013

robust agonist-induced endocytosis, α_{1A}-AR does not [19]. Other reports disagree and suggest that α_{1A}-AR also internalizes upon agonist activation, although to a lesser extent than the α_{1B}-AR, and that α_{1D}-AR is constitutively internalized [12,20]. It has also been suggested that α_{1A}-AR is located in lipid rafts under basal conditions, but exits from these rafts following stimulation, therefore allowing endocytosis [21].

Recently, distinct models of regulation of ERK1/2 activation over time after GPCR activation have been proposed and for many GPCRs, it has been shown that β-arrestin recruitment and receptor-endocytosis are implicated in ERK1/2 activation [22]. For example, angiotensin II activation of the AT_{1A} receptor elicits both, a rapid (peak 2 min), G protein-dependent, ERK1/2 activation and a delayed (peak 5–10 min) and persistent ERK1/2 activation, that is β-arrestin2-dependent [23]. Similar patterns were found for the β_2-AR [24] and the parathyroid hormone receptor [25].

To our knowledge, no coherent analysis of the temporal profile of internalization and ERK1/2 MAPK activation by the three α_1-AR subtypes is available. In the present work, we performed a study of the temporal and spatial patterns of ERK1/2 activation after stimulation of each human α_1-AR stably expressed in HEK293 cells. We explored whether such signals were modified by β-arrestin 2 transcriptional silencing, by blocking receptor endocytosis with concanavalin A (ConA), and by inhibiting PKC with a selective inhibitor. We also studied the different properties of receptor internalization into acidic endosomes by using CypHer5 technology [26,27] and VSV-G epitope tagged receptors to shed light into potential differences between the α_1-AR subtypes.

2. Materials and methods

2.1. Antibodies and reagents

The antibodies used included phospho-p42/44 ERK MAPK (Thr202/ Thr204) and p42/44 ERK MAPK (Cell Signaling Technology, Beverly, MA). CypHer5-anti-VSV-G tag antibody (PA45407), horseradish peroxidase-labeled secondary antibodies and chemiluminescent reagents were from GE Healthcare (Amersham, Buckinghamshire, UK). 4-(2-Hydroxyethyl)piperazine-1-ethanesulfonic acid (HEPES) was purchased from Panreac (Barcelona, Spain). Anti-actin antibody (A2066), concanavalin A (ConA), phenylephrine, Ro 31-8425, prazosin, antibiotic G418, 5-methylurapidil, BMY7378, phentolamine, ethylenediaminetetraacetic acid (EDTA), Nonidet™ P-40, phenylmethanesulfonyl fluoride (PMSF), sodium vanadate, sodium fluoride, ditiothreitol and poly-L-lysine (molecular weight 70,000–150,000) were purchased from Sigma (Sigma, St Louis, MO).

2.2. Construction of the VSV-G-Tagged α_1-AR subtypes

The VSV-G (YTDIEMNRLGK) epitope tag was introduced immediately upstream of each human α_{1A}-AR, α_{1B}-AR and α_{1D}-AR. The amino-terminal primer (5′-AAAAAAAAGGATCCGCCACCATGTACACCGATATAG AGATGAACAGGCTGGGAAAGGTGTTTCTCTCGGGAAATGC-3′) or (5′-AAA AAAAGCTTCCACCATGTACACTGATATCGAAATGAACCGCCTGGGTAAGAA TCCCGACCTGGACACCG-3′) or (5′-AAAAAAAGCTTCCACCATGTACACTG ATATCGAAATGAACCGCCTGGGTAAGACTTTCCGCGATCTCCTGAGCG-3′) was used to incorporate a VSV-G tag, a consensus Kozak sequence and BamHI, HindIII and HindIII sites for α_{1A}-, α_{1B}- and α_{1D}-AR, respectively. Depending on the subtype used as a template, the following carboxyl terminal reverse primer was hybridized: α_{1A}-AR, 5′-AAAAAAAACTCG AGCTAGACTTCCTCCCCGTTC-3′; α_{1B}-AR, 5′AAAAAGAATTCCTAAAACTG CCCGGGCGC-3′; and α_{1D}-AR, 5′-AAAAAGAATTCTTAAATATCGGTCTCCC GTAGGTTGC-3′ respectively, incorporating a XhoI site, EcoRI and EcoRI sites downstream of the coding sequence. All the PCR fragments were subsequently cloned into the plasmid pcDNA3 (Invitrogen, Paisley, Renfrewshire, UK) by in-frame ligation. Construct sequences were confirmed by nucleotide sequencing.

2.3. Cell culture and transfection

HEK293 cells were grown in Dulbecco's modified Eagle's minimum essential medium (Sigma) supplemented with 10% newborn calf serum (Gibco BRL, Gaithersburg, MD), L-glutamine 2 mM (Gibco BRL), 100 μg/ml streptomycin and 100 units/ml penicillin at 37 °C in a humidified atmosphere of 5% CO_2. Cells were transfected by electroporation (300 V, 50 μs, 2 mm gap) using a Multiporator (Eppendorf AG, Hamburg, Germany). After 48 h, cells were selected with G418 400 μg/ml to identify stably expressing clones. All the experiments were performed at around 75% cell confluence.

2.4. RNA extraction and quantitative reverse-transcription polymerase chain reaction

RNA extraction and quantitative reverse-transcription polymerase chain reaction was performed as previously described [28,29]. The threshold cycle (Ct) values obtained for each gene were referenced to GAPDH and converted into the linear form using the term $2^{-\Delta Ct}$ as a value directly proportional to the copy number of mRNA.

2.5. Saturation binding experiments

Intact HEK293 cells (1.25×10^5, 5×10^5 and 1×10^6) stably transfected with each α_1-AR were incubated in duplicate for 45 min at 25 °C with [^{3}H]prazosin in 50 mM Tris HCl (pH 7.5) in a final volume of 1 ml. Samples were incubated with [^{3}H]prazosin concentrations ranging from 0.01 to 6 nM. The experiments were terminated by rapid filtration through fiberglass filters (Schleicher and Schuell, GF 52) pre-soaked in 0.3% polyethyleneimine using a Brandel cell harvester (M24R). The filters were then washed three times with 4 ml of ice cold 50 mM Tris–HCl buffer (pH 7.5), and filter bound radioactivity was determined by liquid scintillation counting. Nonspecific binding was measured in the presence of 10 μM phentolamine. The binding data were analyzed by non-linear regression using Prism, version 4.0 (Graph Pad Software; San Diego, California, USA) to determine the dissociation constant (K_d), and the maximum number of binding sites (B_{max}) for the saturation data. The saturation data were fitted to hyperbolic functions (one or two sites). The best fit to the one-site or two-sites was evaluated using the F-test ($P < 0.05$).

2.6. β-Arrestin 2 siRNA knockdown

The expression of β-arrestin 2 was silenced using HP validated siRNA duplexes targeting human ARRB2 (Hs_ARRB2_10 siRNA; Catalog no. SI02776928, Qiagen). AllStars non-targeting siRNA (Catalog no. 1027284, Qiagen) was used as negative control. The day before transfection, cells were seeded in 30 mm dishes in regular growth medium without antibiotics and grown overnight. The day of transfection, Lipofectamine™2000 (Invitrogen)-siRNA complexes were prepared in Opti-MEM I reduced serum medium according to manufacturer's protocol. Cells were transfected with either 50 nM β-arrestin 2 siRNAs or non-targeting control siRNA complexes for 6 h followed by replacement with fresh growth medium including antibiotics. Transfected cells were assayed 48 h post-transfection. Suppression of the target gene was confirmed by western blot.

2.7. Real-time imaging of the internalization of the α_1-AR subtypes to acidified endosomes in HEK293 cells

HEK293 cells stably expressing the N-terminal VSV-G tagged human α_{1A}-, α_{1B}- and α_{1D}-AR subtypes were plated onto poly-L-lysine coated sterile coverslips 48 h before experimentation. Live cells were washed three times with cold Krebs-Ringer-Hepes buffer (KRH, 120 mM NaCl, 25 mM HEPES, 4.8 mM KCl, 1.2 mM $MgSO_4$ and 1.3 mM $CaCl_2$ at pH 7.4) at 4 °C and were then incubated with CypHer5E linked

anti-VSV-G antibody (GE Healthcare, Amersham, Buckinghamshire, UK) at 5 μg/ml in KRH buffer at 4 °C for 1 h. After washing with KRH buffer at 4 °C, coverslips were rapidly mounted into a flow chamber bath (Attofluor, Molecular Probes; Eugene, OR), placed on the microscope stage in a 95% air and 5% CO_2 atmosphere at 37 °C. At this time, cells were exposed to control pre-warmed KRH buffer or buffer supplemented either with ConA (250 μg/ml) or prazosin (10 μM) for 30 min. After incubation with the aforementioned solutions, the zero time was set up immediately before adding phenylephrine (100 μM) to the imaging chamber and the system was set to acquire images at 5-min intervals for 15 min. A set of control experiments without additions was performed. A laser-scanning confocal inverted microscope (LEICA TCS SP2 (DM-IRBE), equipped with a 60× oil HCX PL APO (1.32 numerical aperture) objective, was used to acquire images. The excitation wavelength was 633 nm using a helium/neon laser and the emitted fluorescence was detected with a 650 nm long pass filter. Image processing and analysis were carried out using MetaMorph, version 6.1r3 (Universal Imaging Corporation) and the Leica software, v.2.61. Internalization kinetic was quantified at different times, by measuring the intensity of 5 defined line segments in the cytosolic region of the cell. We calculated the normalized signal for each line segments at each time point as Ii/I0, where I0 is the intensity taken before agonist stimulation for each segment. For each experiment, 5–8 cells were quantified. Data represent the mean of more than four independent experiments.

2.8. Preparation of cellular extracts and immunoblotting

HEK293 cells on 60 × 15mm plates were starved for 4 h in serum-free medium. Prior to stimulation with phenylephrine, cells were treated for 30 min with ConA (250 μg/ml) or with Ro 31-8425 (1 μM) for 15 min, where indicated. After stimulation, cells were washed once with cold PBS and lysed by rotating 30 min at 4 °C with 500 μl of RIPA buffer (50 mM HEPES, 150 mM NaCl, 10% glycerol, 1.5 mM $MgCl_2$, 0.1% SDS, 1 mM EGTA, 1% Triton-X 100 and 1% sodium deoxycholate) containing protease inhibitor cocktail (Complete®, Roche Applied Science) and phosphatase inhibitor cocktail (PhosSTOP®, Roche Applied Science). Sonication with a Microson™ XL 2000 Ultrasonic Liquid Processor and storage at −80 °C followed. The protein content was measured by the Bradford method (Bio-Rad, Hercules CA). 15 μg of cellular extracts was incubated with SDS-sample buffer (2% SDS, 60 mM Tris buffer, 5% β-mercaptoethanol, 0.01% bromophenol blue and 10% glycerol) at 40 °C for 30 min, separated on 10% SDS-polyacrylamide gels and transferred to PVDF membranes for immunoblotting. Prior to antibody incubation, membranes were blocked in phosphate-buffered saline with 0.1% Tween 20 (PBST) plus 3% BSA (albumin from bovine serum, Sigma, St Louis, MO). Phospho-p42/44 MAPK (Thr202/ Thr204) and p42/44 MAPK antibodies (Cell Signaling Technology), β-arrestin or the actin antibody (Sigma St Louis, MO) were incubated overnight at 4 °C, 1/500 for the p42/44 MAPK and 1/2500 for actin diluted. Membranes were then washed three times with PBST, incubated with an anti-rabbit IgG horseradish peroxidase-conjugated secondary antibody (GE Healthcare, Amersham Buckinghamshire, UK) at 1/2500 for 45 min at room temperature, and was washed extensively with PBST before chemiluminescent detection was performed using the ECL Western Blotting Detection Reagents (GE Healthcare). Images were captured with an AutoChemi System (uvp Bioimaging Systems. Cambridge, UK), and band intensity was measured using LabWorks Image acquisition and Analysis (Ver. 4.6 uvp Bioimaging Systems, Cambridge, UK).

2.9. Confocal microscopy immunocytochemistry

HEK293 cells on poly-L-lysine coated 35 mm glass bottom dishes were starved for 4 h in serum free medium prior to stimulation. After stimulation, cells were fixed with 6% formaldehyde in PBS. Fixed cells were permeabilized with 0.01% Triton in PBS containing 2% BSA for 90 min, incubated with the phospho-p42/44 MAPK (Thr202/Thr204) antibody (Cell Signaling Technology, 1:200) at room temperature overnight, and repeatedly washed using PBS. Incubation of the secondary antibody Alexa Fluor 488 goat anti-rabbit (Molecular Probes; Eugene, OR, 1:1000) was performed for 20 min at room temperature followed by repeated washes using PBS. Then cells were incubated with Hoechst 33342 (Molecular Probes; Eugene, OR, 1:1000) for 15 min in darkness at room temperature on glass slides using Mowiol reagent 4-88 (Calbiochem, Darmstadt, Germany). Confocal images were obtained on a LEICA TCS SP2 (DM-IRB) laser scanning microscope using either the line 488 nm and emission 510–570 nm filter set for Alexa 488 or the 352 and 364 nm excitation and emission 390–480 nm filter set for Hoechst. A z-series of images was acquired at 2 μm steps to produce individual z-stacks. Interaction of Hoechst and p-ERK signals at the same z-stack was depicted in white by colocalization analysis with the Leica software, v2.61.

2.10. Statistical analysis

The results are presented as the mean ± S.E.M. for n experiments. A statistical analysis was performed by the two-way ANOVA or by the Student's *t*-test (GraphPad Software, Inc., San Diego, CA, USA). Significance was defined as $P < 0.05$.

3. Results

Using real-time RT-PCR, saturation radioligand binding techniques, immunocytochemistry and fluorescent ligands we confirmed that the three α_1-ARs, and the corresponding VSV-G-tagged α_1-ARs, were stably expressed in the HEK293 cell lines generated (Supplemental data 1 and 2). We found different expression levels of the three α_1-AR subtypes, especially remarkable for the α_{1D}-subtype in binding but not in PCR assays. Considering the magnitude of the signals elicited by the agonist and in agreement with previous works [30], we propose that this apparent lower Bmax observed, could be interpreted as a lower binding of the α_{1D} subtype to radioligands and not as a reduced protein expression.

3.1. Subtype-specific kinetic pattern of ERK1/2 activation

ERK1/2 activation in the transfected HEK293 cells was promoted by α_1-AR stimulation by phenylephrine (PE). The ERK1/2 phosphorylation induced by each α_1-AR subtype following addition of PE was completely blocked in the presence of the α_1-AR antagonist prazosin (PZ) (Supplemental data 2A). Furthermore, non-transfected cells showed no ERK1/2 phosphorylation after incubation with PE. The effect of different PE concentrations on ERK1/2 activation resulted in concentration-dependent responses (Supplemental data 2B) that varied for the three subtypes with α_{1A} displaying the lowest sensitivity (pED_{50} α_{1A}-AR: 4.325 ± 0.14; pED_{50} α_{1B}-AR: 6.838 ± 0.12; pED_{50} α_{1D}-AR: 6.153 ± 0.16). This corresponds to previous results found when measuring IP_3 generation, contractile response or intracellular Ca^{2+} increase [4,9,14,28]. We selected 100 μM PE for subsequent experiments to ensure that ERK1/2 phosphorylation by all three α_1-AR subtypes was observed. This high dose of PE has also been used in other studies where the ERK1/2 activation by α_1-ARs was investigated [11,12].

As we have previously reported different kinetic profiles of α_{1A}- and α_{1D}-AR responses when studying contractile properties of blood vessels [13,16], we performed a spatio-temporal analysis to examine if the same was true for α_1-AR subtype activation of ERK1/2. As shown in Fig. 1 or Supplemental data 3 and as previously described, the α_{1D}-, but not the α_{1A}- or α_{1B}-AR shows basal phosphorylation of ERK1/2 [11]. Incubation with PE of cells stably expressing α_{1A}-AR rapidly elicits a fast ERK1/2 activation (peak 1–5 min) followed by a slow and progressive reduction of phospho-ERK1/2, which returned to basal levels

after 1 h of PE incubation. The α_{1B}- and α_{1D}-AR transfected cells underwent a similar initial increase but this was transient and the phospho-ERK1/2 levels were rapidly reduced to basal level. To determine if the α_1-AR subtype profiles corresponded to the differential regulation of ERK1/2 activation previously described [23,25], we studied the early component, potentially G protein-dependent, by blocking PKC with the inhibitor Ro 31-8425 [23], and employing the receptor-internalization inhibitor ConA [29], which is known to inhibit endocytosis-dependent ERK1/2 activation [30]. Although DMSO 0.045%, the vehicle of Ro 31-8425, seems to impair the late (>10 min) p-ERK signal after α_{1A}-AR stimulation (Fig. 2A, Control), pre-treatment with Ro 31-8425 resulted in a dramatic decrease (≈70%) in ERK1/2 activation by PE at early time periods (1–5 min). Fig. 2B shows how pre-treatment of the α_{1A}-AR with ConA, prior to stimulation by PE, resulted in transient ERK1/2 activation, which rapidly decreased after 5 min of agonist treatment and returned to near the basal values after 30 min. Since some studies have revealed that in the case of ERK1/2 activation by AT1A receptor stimulation, a Gαq-coupled receptor, beta-arrestin2 but not beta-arrestin1 mediates G protein-independent ERK1/2 activation [23,31,32], we silenced β-arrestin 2 in cells expressing each α_1-AR subtype (see Supplemental data 4). The kinetic profile of the ERK1/2 signal after β-arrestin 2 knock-down was similar to that observed in the presence of ConA (Fig. 2C), the sustained ERK1/2 phosphorylation mediated by activation of the α_{1A}-AR was significantly affected in cells transfected with β-arrestin2 siRNA.

We performed the same Ro 31-8425, ConA and β-arrestin 2 knock-down treatments on cells expressing α_{1B}-ARs. As Fig. 3A depicts, pre-treatment with the PKC inhibitor blocked ERK1/2 activation by PE over the entire 60 min period studied. In this case, pre-treatment with ConA or β-arrestin 2 knock-down had no effect on ERK1/2 activation by PE (Fig. 3B, C). In the HEK293 cells transfected with α_{1D}-AR, pre-treatment with Ro 31-8425 did not inhibit the early increased phospho-ERK level induced by PE, but extended the period of ERK1/2 phosphorylation because phospho-ERK1/2 levels were higher in the presence of Ro 31-8425 after 10 min of PE incubation (Fig. 4A). Pre-treatment with ConA or β-arrestin 2 siRNA did not modify ERK1/2 phosphorylation kinetics after α_{1D}-AR activation (Fig. 4B, C).

3.2. The subtype-specific distribution pattern of ERK1/2 activation

An increasing number of studies suggest a differential spatial regulation of ERK1/2 when activated by either G protein- or β-arrestin-dependent pathways [23,33,34]. Consensus suggests that ERK1/2 rapidly phosphorylated via G protein-activation, is directed to the nucleus, while ERK1/2 resulting from β-arrestin-mediated activation and scaffolding, exclusively remains in the cytoplasm. Fig. 5A displays confocal images depicting phospho-ERK1/2 localization before (PE 0 min), or 5 and 30 min after PE incubation. Stimulation of α_{1A}-AR with PE for 5 min, resulted in an increment of phospho-ERK1/2 throughout the cell, including the nucleus as this fraction co-localized with Hoechst nuclear staining. After 30 min, a lower signal was observed, which was restricted entirely to the cytoplasm. Stimulation of α_{1B}-AR elicited a similar initial (5 min) and transient increase of phospho-ERK1/2 localized in both the cytosol and nucleus. After 30 min of PE stimulation however, no phospho-ERK1/2 signal was observed. Images of the α_{1D}-AR-transfected cells indicated two main differences from the α_{1A} and α_{1B} subtypes: firstly, unstimulated α_{1D}-AR cells showed higher phospho-ERK1/2 basal levels, thus confirming that α_{1D}-AR constitutively activates ERK1/2 as found by Western blot; and secondly, activated ERK1/2 was only present in the cytosol and not in the nucleus, even after 5 min of PE incubation when the phospho-ERK1/2 level was maximal. Nuclear localization of phospho-ERK after 5 min of PE incubation was assessed by co-localization analysis of the images, where p-ERK

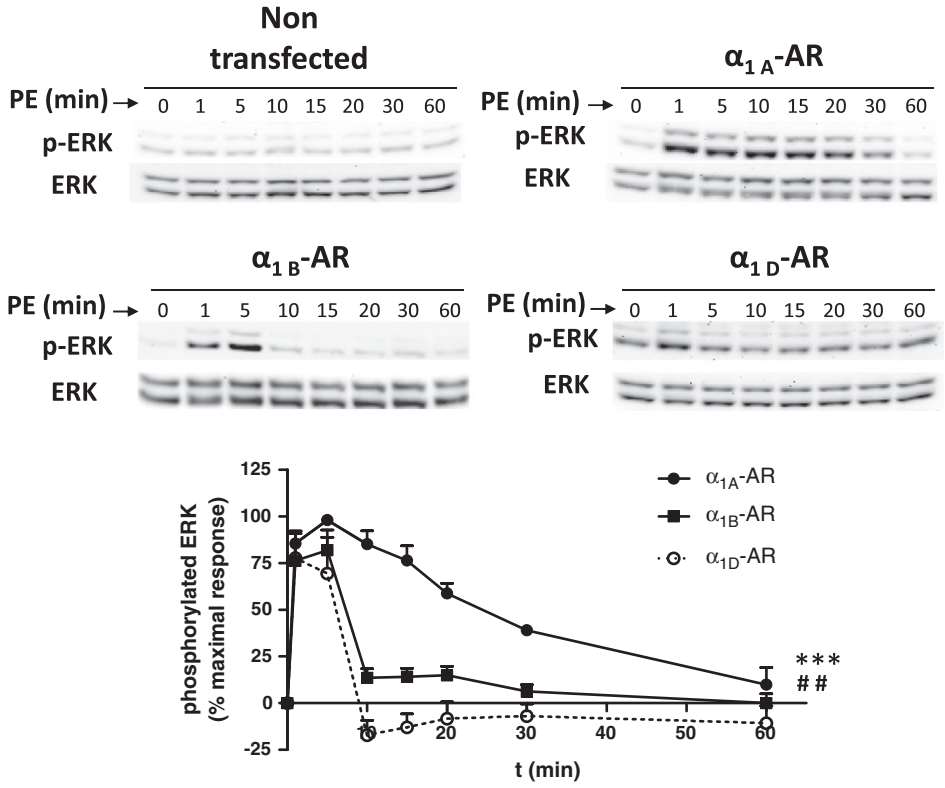

Fig. 1. α_1-AR stimulation shows a subtype-specific pattern of ERK1/2 activation. HEK293 cells not transfected or stably transfected with each α_1-AR subtype were serum-starved for 4 h and stimulated with PE (100 μM) for a 60-min time-course at 37 °C. After stimulation, cellular extracts were prepared as described in "Material and methods". The lower panels show equal amounts of ERK1/2 loaded in each sample. The data represent means ± S.E.M. of 3 independent experiments. Statistics was performed by the two way ANOVA. α_{1A}- vs. α_{1B} or α_{1D}-AR $^{***}P < 0.001$ and α_{1B} vs. α_{1D}-AR $^{\#\#}P < 0.01$.

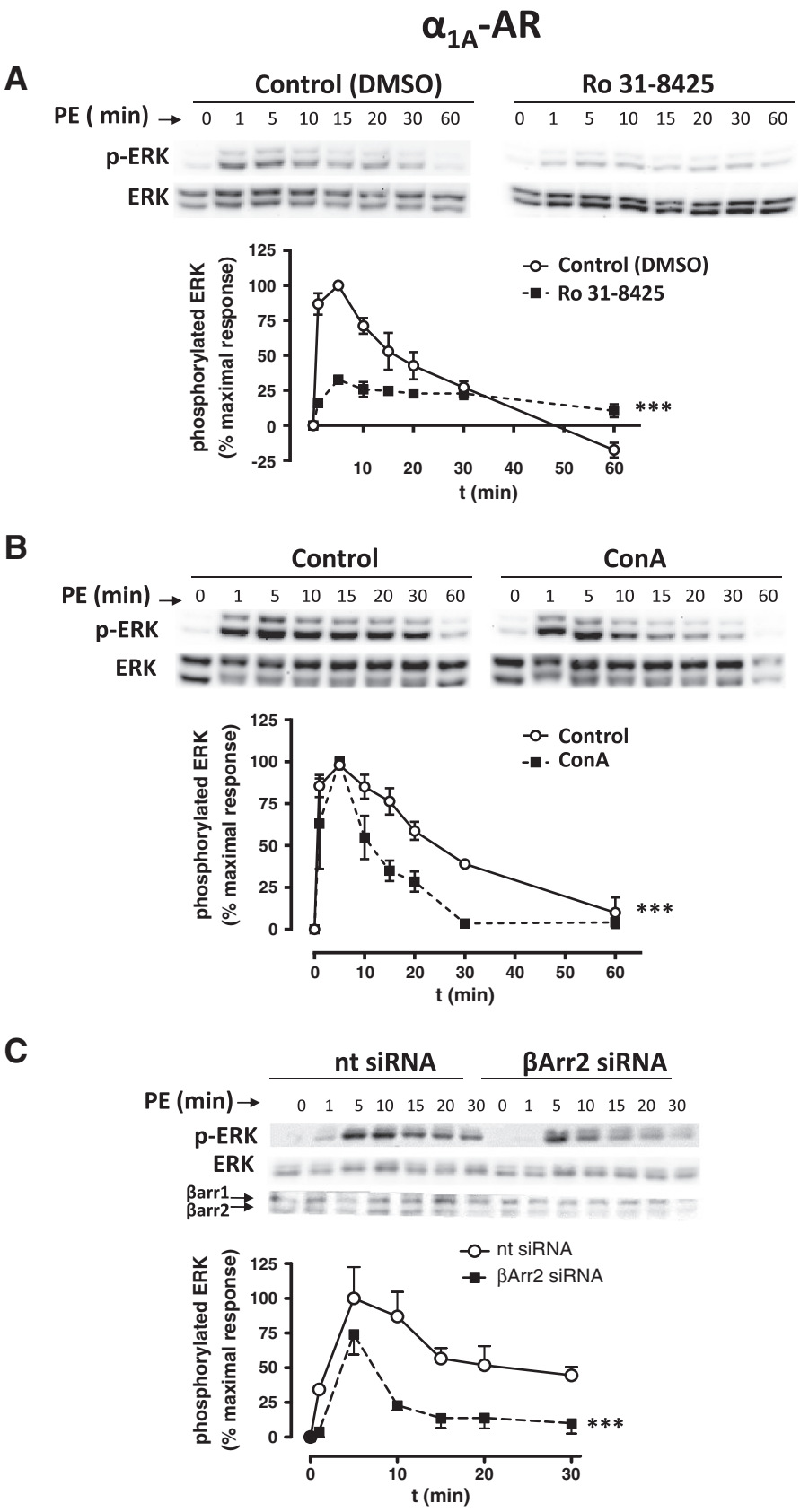

Fig. 2. The PKC inhibitor Ro 31-8425, receptor-internalization inhibitor ConA and β-arrestin2 knock-down modify the PE-induced ERK1/2 activation patterns in cells expressing α_{1A}-AR. 75% confluent HEK293 cells stably expressing the α_{1A}-AR subtype were serum-starved for 4 h and stimulated with PE (100 μM) at 37 °C. When indicated, cells were incubated with A) Me_2SO [Control (DMSO), 0.045%] vehicle or 1 μM Ro 31-8425 for 15 min, B) with ConA 250 μg/ml for 30 min prior to PE stimulation or C) β-arrestin2 was knock-down. The phosphorylated ERK1/2 content in each lane was quantified by densitometry and expressed as a percentage of the maximal ERK1/2 phosphorylation in control. Each data point represents the mean ± S.E.M. of 4–6 independent experiments. Statistics was performed by the two way ANOVA. ***$P < 0.001$ vs. control.

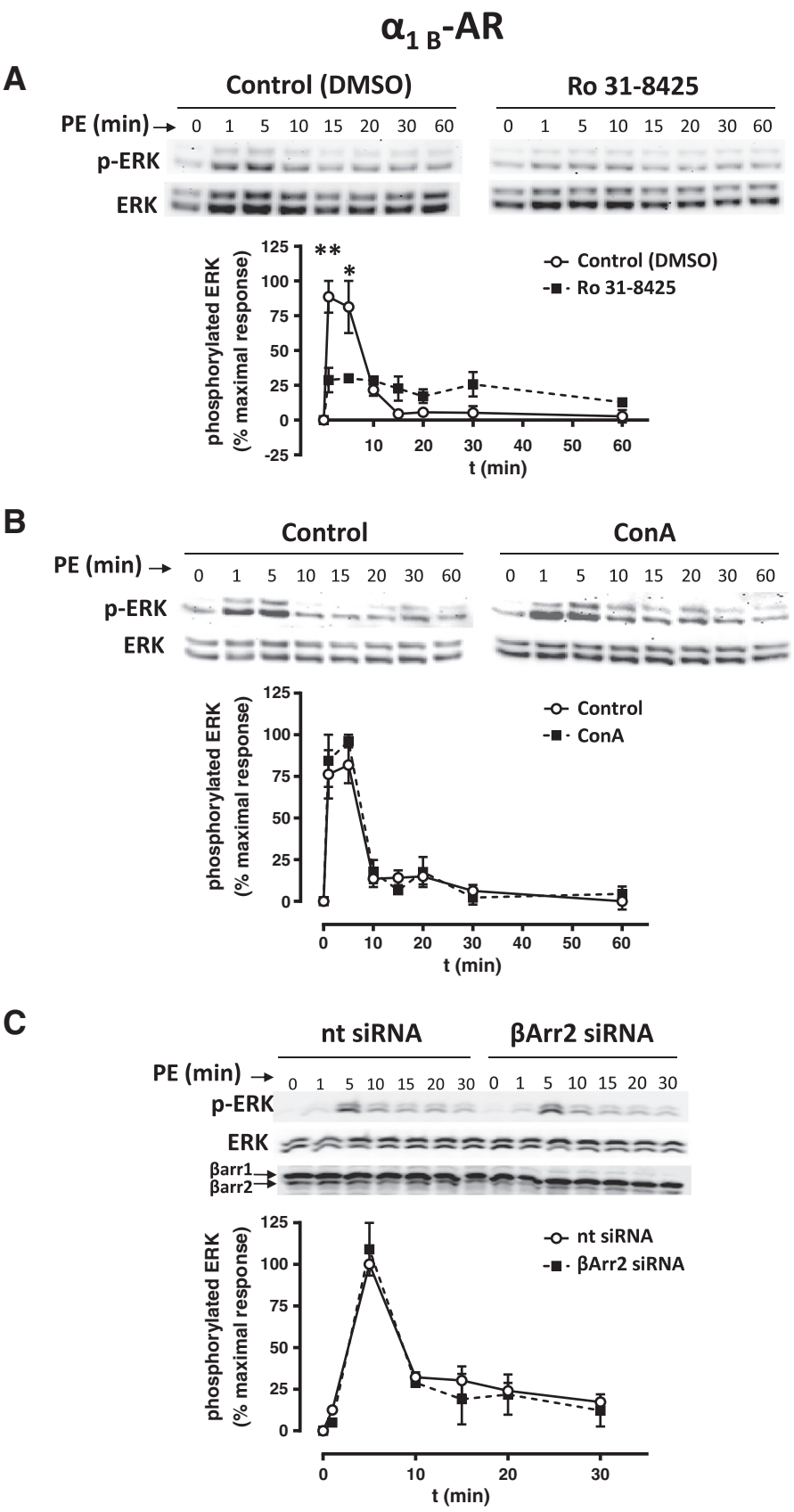

Fig. 3. Ro 31-8425, but not ConA or β-arrestin2 knock-down modifies the PE-induced ERK1/2 activation pattern in the cells expressing α_{1B}-AR. 75% confluent HEK293 cells stably expressing the α_{1B}-AR subtype were serum-starved for 4 h and stimulated with PE (100 μM) at 37 °C. When indicated, cells were incubated with A) Me_2SO [Control (DMSO), 0.045%] vehicle or 1 μM Ro 31-8425 for 15 min, or B) with ConA 250 μg/ml 30 min prior to PE stimulation or C) β-arrestin2 was knock-down. The phosphorylated ERK1/2 content in each lane was quantified by densitometry and expressed as a percentage of the maximal ERK1/2 phosphorylation in control. Each data point represents the mean ± S.E.M. of 3 independent experiments. Statistics was performed by the Student's *t* test. **P < 0.001, *P < 0.05 vs. control.

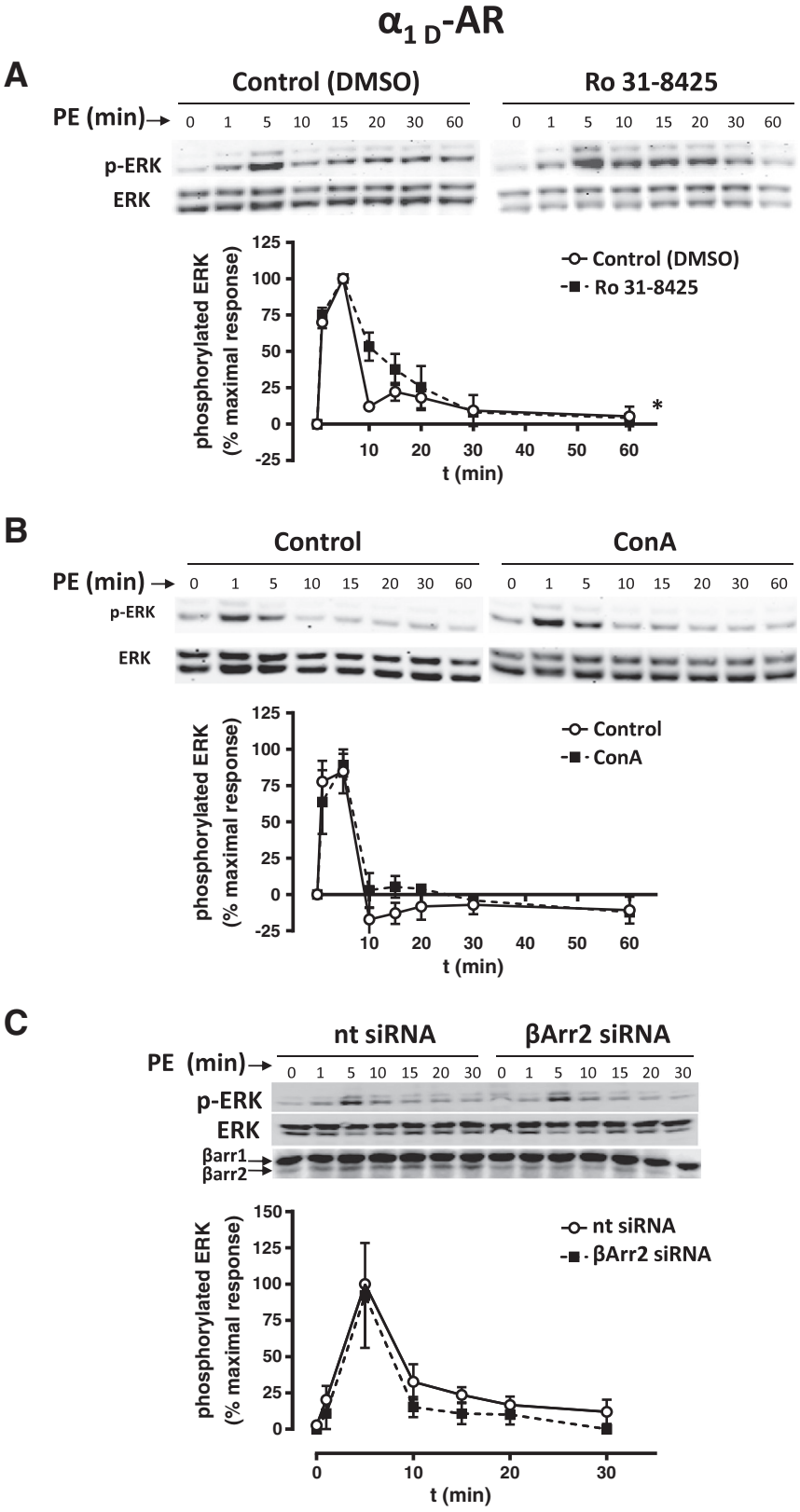

Fig. 4. Ro 31-8425, but not ConA or β-arrestin2 knock-down modifies the PE-induced ERK1/2 activation pattern in the cells transfected with α_{1D}-AR. 75% confluent HEK293 cells stably transfected with the α_{1D}-AR subtype were serum-starved for 4 h and stimulated with PE (100 μM) at 37 °C. When indicated, cells were incubated A) with Me_2SO [Control (DMSO), 0.045%] vehicle or 1 μM Ro-31-8425 for 15 min before PE incubation, B) with ConA 250 μg/ml 30 min prior to PE stimulation or C) β-arrestin2 was knock-down. The phosphorylated ERK1/2 content in each lane was quantified by densitometry and expressed as a percentage of the maximal ERK1/2 phosphorylation in control. Each data point represents the mean ± S.E.M. of 3 independent experiments. Statistics was performed by the two way ANOVA Control vs. Ro 31-8425. *$P < 0.05$.

and Hoechst nuclear staining coexisting at the same level is depicted in white (Fig. 5A).

To determine if the initial phospho-ERK1/2 distribution induced by PE activation (peak 5 min) was PKC-dependent, we performed immunocytochemistry experiments following incubation with the PKC inhibitor Ro 31-8425 before PE stimulation. Although DMSO could slightly modify p-ERK localization to the nucleus after PE 5 min when compared to stimulus without DMSO, Fig. 5B shows confocal images demonstrating that PKC inhibition prevented phospho-ERK1/2 translocation to the nucleus in the α_{1A}- and α_{1B}-AR-transfected cells. By contrast, Ro 31-8425 had no effect on either the phospho-ERK1/2 localization after α_{1D}-AR activation or on the 30-min PE-induced ERK1/2 phosphorylation produced via the α_{1A}-AR subtype.

3.3. Subtype-specific receptor internalization patterns

By N-terminally tagging the three α_1-AR subtypes with the VSV-G epitope and employing a CypHer-5 dye labeled anti-VSV-G antibody that displays red fluorescence only in an acidic environment [26,27], internalization to the acidified endosomes of previously cell surface receptors was monitored in stably transfected, live HEK293 cells. Initially, we localized the three subtypes of α_1-ARs by confocal microscopy as previously described [11,12] (Supplemental data 5) and verified that the VSV-G-tagged α_1-ARs activated ERK1/2 with the same kinetics as the non tagged receptors, this is the VSV-G-α_{1A}-AR elicits an early and late ERK1/2 activation, while the VSV-G-α_{1B}- and VSV-G-α_{1D}-AR only activate ERK1/2 after 5 min but not after 30 min (Supplemental

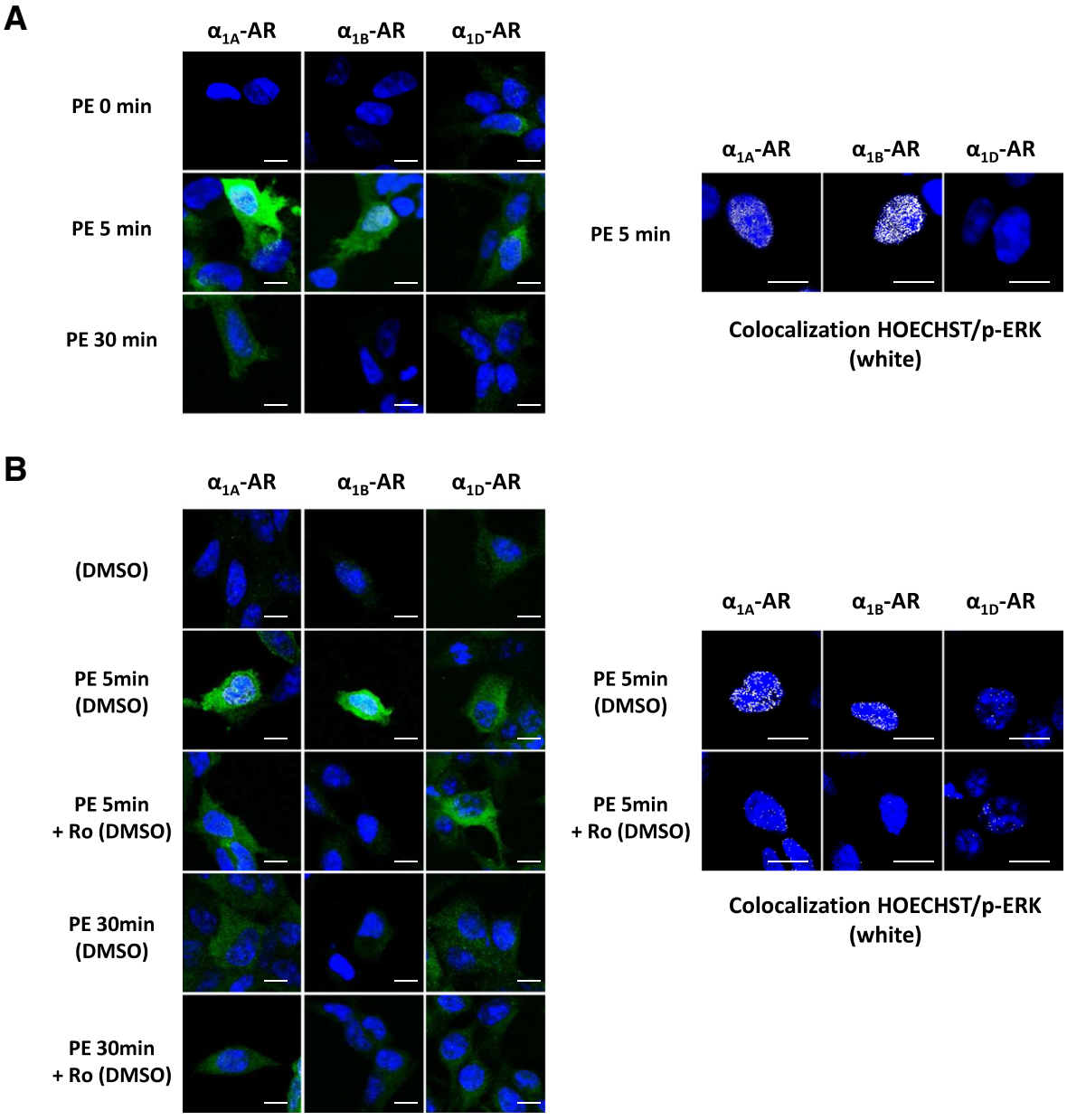

Fig. 5. α_1-AR stimulation shows a subtype-specific distribution pattern of ERK1/2 activation. 75% confluent HEK293 cells stably expressing each α_1-AR subtype were serum-starved for 4 h and stimulated with PE (100 μM) for 0, 5 and 30 min at 37 °C. These were A) not pretreated with Ro 31-8425 or B) pretreated with Ro 31-8425 15 min before PE addition and vehicle (DMSO). After stimulation, cells were prepared for immunocytochemistry as described under the "Material and methods". Colocalization of p-ERK (green) and Hoechst-stain nuclei (blue) is represented by white in the overlay image. Bar scale represents 10 μm.

data 6). Both VSV-G-α_{1A}- and VSV-G-α_{1B}-AR, underwent constitutive (Fig. 6A) and agonist-induced internalization (Fig. 6B and C) to acidic endosomes. According to our experimental procedure, after 30 min of incubation at 37 °C we can observe that the constitutive internalization to endosomes of VSV-α_{1B}-AR, was inhibited by ConA (Fig. 6A), an inhibitor of receptor-endocytosis [35–38]. The phenylephrine induced internalization of VSV-G-α_{1A} but not that of the VSV-α_{1B} subtype (Fig. 6B and C), was decreased by ConA. We were not able to detect the internalization of the VSV-G-α_{1D}-AR to acidified endosomes using this approach (results not shown).

4. Discussion

Some recent studies have shown that after the stimulation of GPCRs, such as the angiotensin AT_{1A} receptor [23], β_2-AR [24] and parathyroid hormone receptors [25], a pool of ERK1/2 that is activated by the G protein-dependent pathway translocates into the nucleus, whereas activated ERK1/2 that is dependent on β-arrestin-mediated receptor endocytosis, remains in the cytoplasm [23,33,34]. In this work, we have characterized a rapid phosphorylation of ERK1/2 that is dependent on α_{1A}- and α_{1B}-AR activation of PKC, and promotes p-ERK1/2 translocation to the nucleus.

Furthermore, we have also shown that α_{1A}-, but not α_{1B}-AR, elicits a sustained activation of ERK1/2 which limits its distribution to the cytoplasm and which is inhibited by β-arrestin 2 knockdown and blocked by the receptor endocytosis-inhibitor ConA, suggesting that the internalized receptor plays a functional role in this signaling process. Distinct expression levels of α_{1A}- and α_{1B}-AR could be involved in the differences observed in the time-course of ERK1/2 activation. However, the fact that response was expressed as a percentage of the maximal response in each case minimizes the distortion introduced by the different expression level. In addition, confirming our results, a similar α_{1A}-dependent activation of ERK1/2 through an endocytic pathway has been recently evidenced in HEK293 cells [39]. Present results show for the first time that the biphasic ERK phosphorylation pattern described for certain GPCRs has been attributed only to the α_{1A}-subtype and, what is more, that the three different α_1-AR subtypes present significant differences in this regard (shown schematically in Fig. 7). Along these lines, we have demonstrated that α_{1B}-AR elicits a rapid, transient ERK activation, which is PKC-dependent and delivered to the nucleus, but did not show the β-arrestin dependent ERK phosphorylation

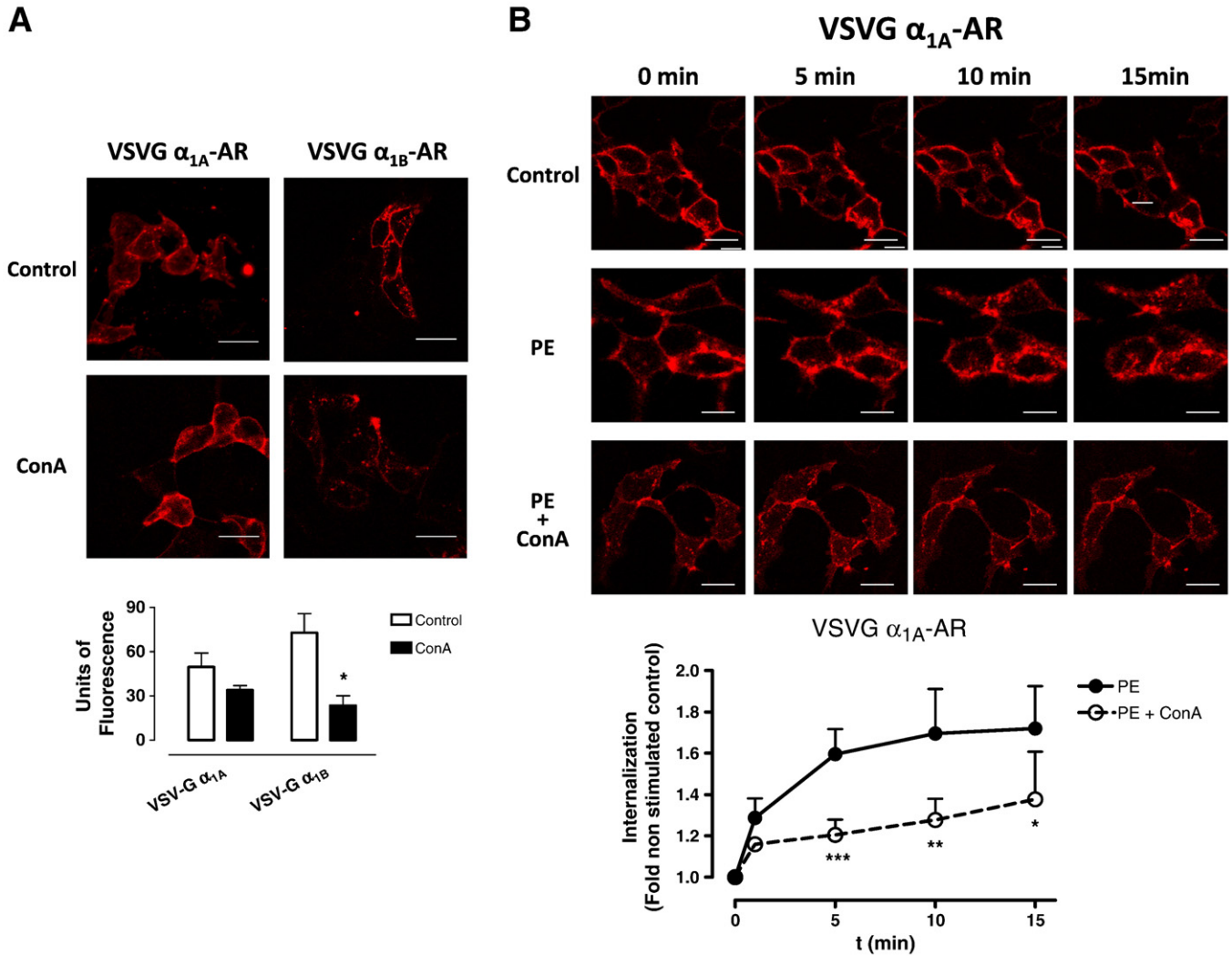

Fig. 6. α_{1A}- and α_{1B}-AR stimulations show a subtype-specific receptor-internalization pattern and dependency on ConA. 75% confluent HEK293 cells stably transfected with VSV-G-tagged-α_{1A}- or VSV-G-tagged-α_{1B}-AR were incubated with the CyPher5 linked anti-VSV antibody at 5 μg/ml for 1 h. After washing with the KRH buffer, cells were mounted in a flow chamber bath and placed in a confocal microscope stage in a 95% air and 5% CO_2 atmosphere at 37 °C. At this time, cells were pre-warmed with the KRH buffer supplemented or not supplemented with ConA (250 μg/ml) for 30 min and the constitutive internalization was measured (A). At this point, phenylephrine (PE) 100 μM was added and agonist-induced internalization of α_{1A} and α_{1B} -ARs was quantified for 30 min (B and C respectively) as described in "Material and methods". Statistics was performed by two way ANOVA ($P < 0.05$) and by Student's *t*-test to compare internalization at each time. ***$P < 0.001$, **$P < 0.01$, and *$P < 0.05$ vs. control or PE. Bar scale represents 20 μm.

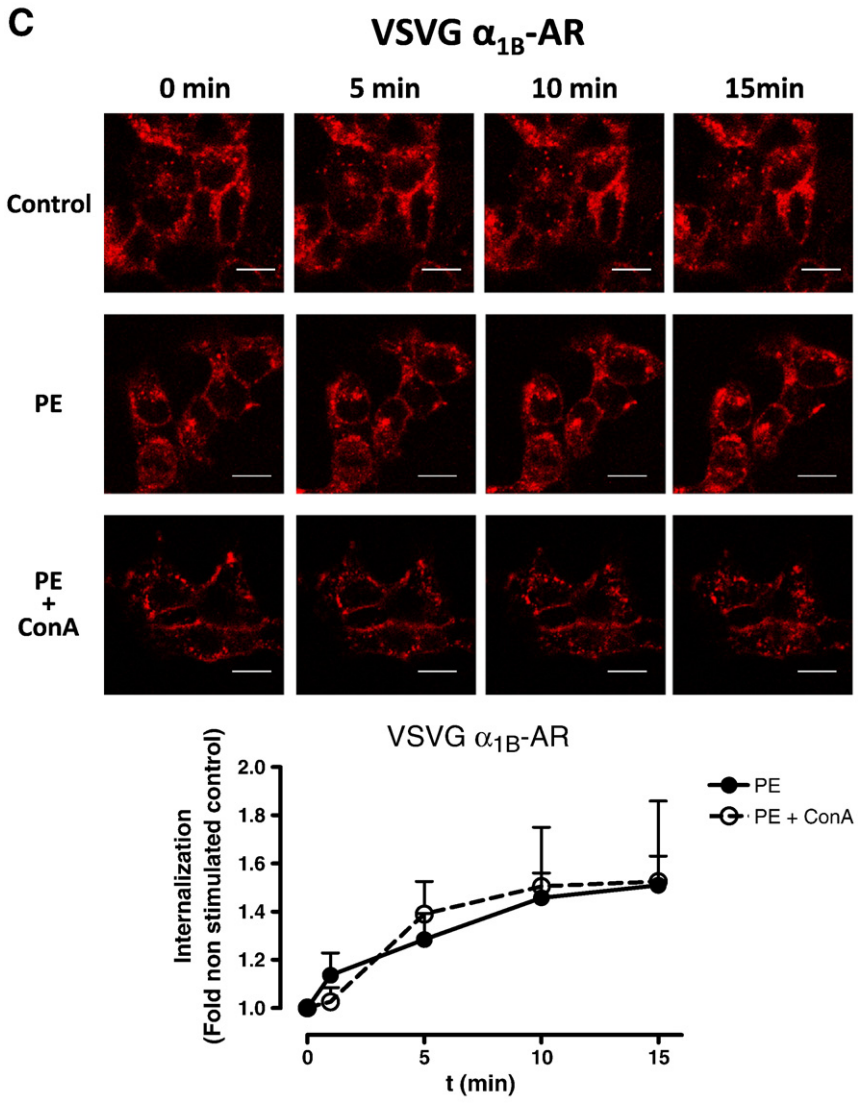

Fig. 6 (*continued*).

observed with the α_{1A}-subtype. Although α_{1D}-AR also shows an early, transient ERK activation after agonist stimulation, this initial peak is not only independent of PKC and β-arrestin, but is also confined to the cytosol, which therefore increases the complexity of the α_1-AR signaling network. Exactly why α_{1D}-AR activates ERK through a distinct pathway is an open question that needs to be investigated further.

At this point, it is interesting to note that both the α_{1A} and α_{1B} receptors internalize upon agonist activation but ConA, a well-known receptor-internalization blocker [35–38], only abolishes agonist-mediated internalization of α_{1A}-AR. When we analyzed the internalization together to ERK phosphorylation kinetics elicited by either α_{1A}- or α_{1B}-AR, we found that maximal α_{1A}-AR internalization was achieved 5 min after PE stimulation but a sustained ERK activation located in the cytosol and inhibited by β-arrestin 2 knockdown and ConA was observed even when the receptor was maximally internalized. Conversely, agonist induced internalization of the α_{1B}-AR, by a mechanism that, in our experimental conditions, is unaffected by β-arrestin 2 knockdown or treatment with ConA, was almost maximal at 10 min but, at this time, ERK1/2 phosphorylation had already returned to basal levels, suggesting that the internalized receptor was not able to activate ERK1/2. All these findings suggest that α_{1A}-AR, when stimulated by PE, internalizes via a ConA-sensitive mechanism responsible for the late PKC-independent ERK activation and this relates to the anti-apoptotic activity of the α_{1A} subtype. Thus, differences in the internalization mechanisms lead to different intracellular signaling pathways for each subtype, which could explain why anti-apoptotic activity, could be exhibited only by the α_{1A} subtype. In this regard, it has been previously found that the α_{1B}-subtype shows a stronger interaction with β-arrestin than the α_{1A}-AR [19]. Our results are compatible with these previous observations. In our hands, the constitutive internalization of the α_{1B}-subtype was inhibited by ConA, but the subsequent addition of the agonist gives a similar profile of internalization independent of the presence of ConA, suggesting that receptor-internalization of the α_{1B}-AR was, at this time, completed. Therefore, it would be interesting to further study the different mechanisms of internalization in order to establish why the α_{1A}-AR, which shows a weaker interaction with β-arrestin, elicits a late ERK1/2 activation dependent on endosomic internalization, while the α_{1B}-AR does not.

Little is known about the role of a differential ERK distribution in the cell. Nuclear p-ERK substrates, particularly transcription factors, have been extensively studied but cytoplasmic substrates have been the object of less scrutiny. However, several examples suggest that cytoplasmic ERK activity is important in cell viability and apoptosis [40,41] and it has been established that the cyto-protective activity of other GPCR as AT_{1A} receptors is related to β-arrestin 2 dependent activation of cytosolic ERK. In the same way, perinuclearly localized

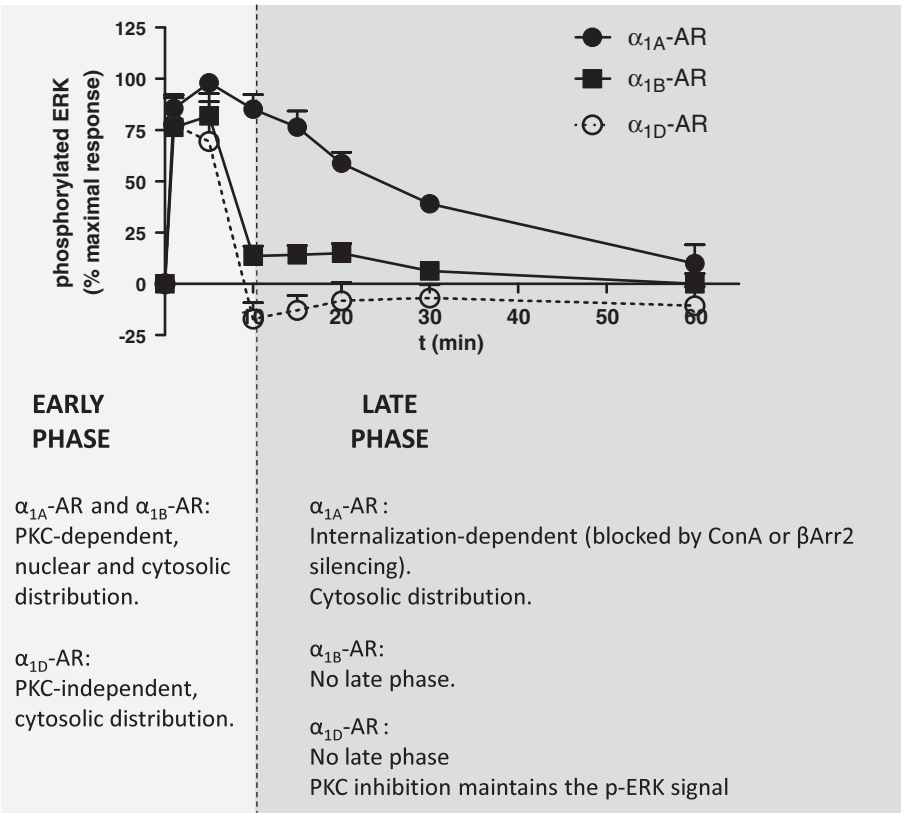

Fig. 7. Scheme depicting the different pathways involved in ERK1/2 phosphorylation by the three human α_1-AR subtypes. PKC, protein kinase C.

α_{1A} -ARs, but not α_{1B} or α_{1D}-AR, has been shown that exerts an antiapoptotic and cardioprotective role in cardiomyocytes, which is mediated by ERK activation [42].

On the other hand, it has been recently shown that the wild-type and a genetic variant of the α_{1A}-AR transactivate EGFR via a β-arrestin-dependent mechanism [43]. The parallelism between this mechanism and the β_1-AR mediated EGFR transactivation, which confers cardioprotection [44,45] suggests that EGFR transactivation could be involved in the antiapoptotic and cardioprotective activity of the α_{1A}-subtype.

Therefore, previous evidences and present results strongly suggest that the cytosolic-confined pool of p-ERK activated by α_{1A}-AR in a G protein-independent β-arrestin dependent fashion, probably via EGFR transactivation [43], is a prosurvival pathway relevant for cardioprotection, and could explain the clinical evidence that chronic use of non subtype selective α_1 antagonists as doxazosin was associated with higher risk factor for coronary heart disease [46,47]. Future work in the field could be necessary to establish the exact role of EGFR transactivation on the G protein-independent, β-arrestin dependent retention of p-ERK in the cytoplasm elicited by α_{1A}-AR activation.

Previous studies have identified constitutive activity of α_{1D}-AR; that is, activity in the absence of agonist stimulus [11,13–16]. In order to analyze potential constitutive activation of ERK1/2, we compared basal phosphorylation state in the cells transfected with each α_1-AR subtype. As Supplemental Fig. 3 shows, α_{1D}-AR-transfected cells showed the highest phospho-ERK1/2 basal level and treatment with α_1-antagonists such as prazosin (PZ, a non selective α_1 antagonist) and BMY 7378 (a selective α_{1D} antagonist), decreased this basal ERK1/2 phosphorylation, thus confirming that α_{1D}-AR constitutively activates ERK1/2 and that these compounds act as inverse agonists, as previously concluded [11,13–16]. Unfortunately, we were not able to observe internalization of α_{1D}-AR using CypHer5 technology and the VSV-G-tagged receptor. As previously described, α_{1D}-AR is intracellularly distributed [12] and has shown striking difficulties when attempts to detect it have been made [48]. We hypothesize two reasons why we were not able to detect VSV-G-tagged α_{1D}-AR: first, a CypHer-5-antiVSV-G-tagged receptor is visible only in the acidic pH environment of an internalized endosome [26], meaning that active internalization is needed to visualize the receptor. If α_{1D}-AR is predominantly intracellular it would not be labeled by the antibody and detected by the CypHer5 dye. In fact, previous works strongly suggest that the α_{1D}-AR is constitutively active and, as a result, is localized to intracellular compartments involving β-arrestin2 internalization [11]. Second, it is possible that the trafficking pattern of VSV-G-α_{1D}-AR could be modified by VSV-G-tagging, because the characteristic distribution of α_{1D}-AR appears to be related to its long N-terminal domain [49], where the VSV-G-tag is placed.

Additional experiments are required to clarify this point, as well as the physiological meaning of both the constitutive and PE-induced ERK1/2 phosphorylation mediated by the α_{1D}-AR that is not dependent on PKC activation and is restricted to the cytosol.

5. Conclusions

The present study reveals that the three α_1-AR subtypes present different spatio-temporal patterns of ERK phosphorylation and receptor internalization. Only α_{1A}-AR elicits a late and sustained ERK phosphorylation that is dependent on receptor-internalization and is restricted to the cytosol. This late ERK activation may relate to the anti-apoptotic-cardioprotective effect of α_{1A}-AR.

Acknowledgements

This study was supported by research grants from the Instituto de Salud Carlos III, Fondo de Investigaciones Sanitarias (FIS PI070509) and Generalitat Valenciana (GRUPOS05-038 and GVACOMP2009/261).

Appendix A. Supplementary data

Supplementary data to this article can be found online at http://dx.doi.org/10.1016/j.bbamcr.2013.06.013.

References

[1] D. Wu, A. Katz, C.H. Lee, M.I. Simon, Activation of phospholipase C by alpha 1-adrenergic receptors is mediated by the alpha subunits of Gq family, J. Biol. Chem. 267 (1992) 25798–25802.

[2] M.W. Lee, D.L. Severson, Signal transduction in vascular smooth muscle: diacylglycerol second messengers and PKC action, Am. J. Physiol. 267 (1994) C659–C678.

[3] D.M. Perez, M.B. DeYoung, R.M. Graham, Coupling of expressed alpha 1B- and alpha 1D-adrenergic receptor to multiple signaling pathways is both G protein and cell type specific, Mol. Pharmacol. 44 (1993) 784–795.

[4] T.L. Theroux, T.A. Esbenshade, R.D. Peavy, K.P. Minneman, Coupling efficiencies of human alpha 1-adrenergic receptor subtypes: titration of receptor density and responsiveness with inducible and repressible expression vectors, Mol. Pharmacol. 50 (1996) 1376–1387.

[5] J.L. Benovic, H. Kuhn, I. Weyand, J. Codina, M.G. Caron, R.J. Lefkowitz, Functional desensitization of the isolated beta-adrenergic receptor by the beta-adrenergic receptor kinase: potential role of an analog of the retinal protein arrestin (48-kDa protein), Proc. Natl. Acad. Sci. U. S. A. 84 (1987) 8879–8882.

[6] S. Keffel, A. Alexandrov, M. Goepel, M.C. Michel, Alpha(1)-adrenoceptor subtypes differentially couple to growth promotion and inhibition in Chinese hamster ovary cells, Biochem. Biophys. Res. Commun. 272 (2000) 906–911.

[7] S.S. Ferguson, Evolving concepts in G protein-coupled receptor endocytosis: the role in receptor desensitization and signaling, Pharmacol. Rev. 53 (2001) 1–24.

[8] O.B. Goodman Jr., J.G. Krupnick, F. Santini, V.V. Gurevich, R.B. Penn, A.W. Gagnon, J.H. Keen, J.L. Benovic, Beta-arrestin acts as a clathrin adaptor in endocytosis of the beta2-adrenergic receptor, Nature 383 (1996) 447–450.

[9] M.T. Piascik, D.M. Perez, Alpha1-adrenergic receptors: new insights and directions, J. Pharmacol. Exp. Ther. 298 (2001) 403–410.

[10] H. Zhong, K.P. Minneman, Alpha1-adrenoceptor subtypes, Eur. J. Pharmacol. 375 (1999) 261–276.

[11] D.F. McCune, S.E. Edelmann, J.R. Olges, G.R. Post, B.A. Waldrop, D.J. Waugh, D.M. Perez, M.T. Piascik, Regulation of the cellular localization and signaling properties of the alpha(1B)- and alpha(1D)-adrenoceptors by agonists and inverse agonists, Mol. Pharmacol. 57 (2000) 659–666.

[12] D. Chalothorn, D.F. McCune, S.E. Edelmann, M.L. Garcia-Cazarin, G. Tsujimoto, M.T. Piascik, Differences in the cellular localization and agonist-mediated internalization properties of the alpha(1)-adrenoceptor subtypes, Mol. Pharmacol. 61 (2002) 1008–1016.

[13] R. Gisbert, Y. Madrero, V. Sabino, M.A. Noguera, M.D. Ivorra, P. D'Ocon, Functional characterization of alpha 1-adrenoceptor subtypes in vascular tissues using different experimental approaches: a comparative study, Br. J. Pharmacol. 138 (2003) 359–368.

[14] R. Gisbert, M.A. Noguera, M.D. Ivorra, P. D'Ocon, Functional evidence of a constitutively active population of alpha(1D)-adrenoceptors in rat aorta, J. Pharmacol. Exp. Ther. 295 (2000) 810–817.

[15] M.A. Noguera, M.D. Ivorra, P. D'Ocon, Functional evidence of inverse agonism in vascular smooth muscle, Br. J. Pharmacol. 119 (1996) 158–164.

[16] K. Ziani, R. Gisbert, M.A. Noguera, M.D. Ivorra, P. D'Ocon, Modulatory role of a constitutively active population of alpha(1D)-adrenoceptors in conductance arteries, Am. J. Physiol. Heart Circ. Physiol. 282 (2002) H475–H481.

[17] J.A. Garcia-Sainz, M.E. Torres-Padilla, Modulation of basal intracellular calcium by inverse agonists and phorbol myristate acetate in rat-1 fibroblasts stably expressing alpha1d-adrenoceptors, FEBS Lett. 443 (1999) 277–281.

[18] R. Gisbert, F. Perez-Vizcaino, A.L. Cogolludo, M.A. Noguera, M.D. Ivorra, J. Tamargo, P. D'Ocon, Cytosolic Ca2+ and phosphoinositide hydrolysis linked to constitutively active alpha 1D-adrenoceptors in vascular smooth muscle, J. Pharmacol. Exp. Ther. 305 (2003) 1006–1014.

[19] L. Stanasila, L. Abuin, J. Dey, S. Cotecchia, Different internalization properties of the alpha1a- and alpha1b-adrenergic receptor subtypes: the potential role of receptor interaction with beta-arrestins and AP50, Mol. Pharmacol. 74 (2008) 562–573.

[20] D.P. Morris, R.R. Price, M.P. Smith, B. Lei, D.A. Schwinn, Cellular trafficking of human alpha1a-adrenergic receptors is continuous and primarily agonist-independent, Mol. Pharmacol. 66 (2004) 843–854.

[21] D.P. Morris, B. Lei, Y.X. Wu, G.A. Michelotti, D.A. Schwinn, The alpha1a-adrenergic receptor occupies membrane rafts with its G protein effectors but internalizes via clathrin-coated pits, J. Biol. Chem. 283 (2008) 2973–2985.

[22] Y. Daaka, L.M. Luttrell, S. Ahn, G.J. Della Rocca, S.S. Ferguson, M.G. Caron, R.J. Lefkowitz, Essential role for G protein-coupled receptor endocytosis in the activation of mitogen-activated protein kinase, J. Biol. Chem. 273 (1998) 685–688.

[23] S. Ahn, S.K. Shenoy, H. Wei, R.J. Lefkowitz, Differential kinetic and spatial patterns of beta-arrestin and G protein-mediated ERK activation by the angiotensin II receptor, J. Biol. Chem. 279 (2004) 35518–35525, (%20).

[24] S.K. Shenoy, M.T. Drake, C.D. Nelson, D.A. Houtz, K. Xiao, S. Madabushi, E. Reiter, R.T. Premont, O. Lichtarge, R.J. Lefkowitz, Beta-arrestin-dependent, G protein-independent ERK1/2 activation by the beta2 adrenergic receptor, J. Biol. Chem. 281 (2006) 1261–1273.

[25] D. Gesty-Palmer, M. Chen, E. Reiter, S. Ahn, C.D. Nelson, S. Wang, A.E. Eckhardt, C.L. Cowan, R.F. Spurney, L.M. Luttrell, R.J. Lefkowitz, Distinct beta-arrestin- and G protein-dependent pathways for parathyroid hormone receptor-stimulated ERK1/2 activation, J. Biol. Chem. 281 (2006) 10856–10864.

[26] E.J. Adie, M.J. Francis, J. Davies, L. Smith, A. Marenghi, C. Hather, K. Hadingham, N.P. Michael, G. Milligan, S. Game, CypHer 5: a generic approach for measuring the activation and trafficking of G protein-coupled receptors in live cells, Assay Drug Dev. Technol. 1 (2003) 251–259.

[27] E.J. Adie, S. Kalinka, L. Smith, M.J. Francis, A. Marenghi, M.E. Cooper, M. Briggs, N.P. Michael, G. Milligan, S. Game, A pH-sensitive fluor, CypHer 5, used to monitor agonist-induced G protein-coupled receptor internalization in live cells, Biotechniques 33 (2002) 1152–1157.

[28] K. Taguchi, M. Yang, M. Goepel, M.C. Michel, Comparison of human alpha1-adrenoceptor subtype coupling to protein kinase C activation and related signalling pathways, Naunyn Schmiedebergs Arch. Pharmacol. 357 (1998) 100–110.

[29] J.D. Pediani, J.F. Colston, D. Caldwell, G. Milligan, C.J. Daly, J.C. McGrath, Beta-arrestin-dependent spontaneous alpha1a-adrenoceptor endocytosis causes intracellular transportation of alpha-blockers via recycling compartments, Mol. Pharmacol. 67 (2005) 992–1004.

[30] L.M. Luttrell, Y. Daaka, G.J. Della Rocca, R.J. Lefkowitz, G protein-coupled receptors mediate two functionally distinct pathways of tyrosine phosphorylation in rat 1a fibroblasts. Shc phosphorylation and receptor endocytosis correlate with activation of Erk kinases, J. Biol. Chem. 272 (1997) 31648–31656.

[31] S. Ahn, H. Wei, T.R. Garrison, R.J. Lefkowitz, Reciprocal regulation of angiotensin receptor-activated extracellular signal-regulated kinases by beta-arrestins 1 and 2, J. Biol. Chem. 279 (2004) 7807–7811.

[32] H. Wei, S. Ahn, S.K. Shenoy, S.S. Karnik, L. Hunyady, L.M. Luttrell, R.J. Lefkowitz, Independent beta-arrestin 2 and G protein-mediated pathways for angiotensin II activation of extracellular signal-regulated kinases 1 and 2, Proc. Natl. Acad. Sci. U.S. A. 100 (19) (2003) 10782–10787.

[33] K.A. DeFea, J. Zalevsky, M.S. Thoma, O. Dery, R.D. Mullins, N.W. Bunnett, beta-arrestin-dependent endocytosis of proteinase-activated receptor 2 is required for intracellular targeting of activated ERK1/2, J. Cell Biol. 148 (2000) 1267–1281.

[34] A. Tohgo, K.L. Pierce, E.W. Choy, R.J. Lefkowitz, L.M. Luttrell, Beta-arrestin scaffolding of the ERK cascade enhances cytosolic ERK activity but inhibits ERK-mediated transcription following angiotensin AT1a receptor stimulation, J. Biol. Chem. 277 (2002) 9429–9436.

[35] J.A. Gray, D.J. Sheffler, A. Bhatnagar, J.A. Woods, S.J. Hufeisen, J.L. Benovic, B.L. Roth, Cell-type specific effects of endocytosis inhibitors on 5-hydroxytryptamine(2A) receptor desensitization and resensitization reveal an arrestin-, GRK2-, and GRK5-independent mode of regulation in human embryonic kidney 293 cells, Mol. Pharmacol. 60 (2001) 1020–1030.

[36] A. Mashukova, M. Spehr, H. Hatt, E.M. Neuhaus, Beta-arrestin2-mediated internalization of mammalian odorant receptors, J. Neurosci. 26 (2006) 9902–9912.

[37] C.H. So, V. Verma, B.F. O'Dowd, S.R. George, Desensitization of the dopamine D1 and D2 receptor hetero-oligomer mediated calcium signal by agonist occupancy of either receptor, Mol. Pharmacol. 72 (2007) 450–462.

[38] Q. Zhang, M. Hong, P. Duan, Z. Pan, J. Ma, G. You, Organic anion transporter OAT1 undergoes constitutive and protein kinase C-regulated trafficking through a dynamin- and clathrin-dependent pathway, J. Biol. Chem. 283 (2008) 32570–32579.

[39] F. Liu, K. He, X. Yang, N. Xu, Z. Liang, M. Xu, X. Zhao, Q. Han, Y. Zhang, Alpha1A-adrenergic receptor induces activation of extracellular signal-regulated kinase 1/2 through endocytic pathway, PLoS One 6 (2011) e21520.

[40] K. Breitschopf, J. Haendeler, P. Malchow, A.M. Zeiher, S. Dimmeler, Posttranslational modification of Bcl-2 facilitates its proteasome-dependent degradation: molecular characterization of the involved signaling pathway, Mol. Cell. Biol. 20 (2000) 1886–1896.

[41] J. Garcia, Y. Ye, V. Arranz, C. Letourneux, G. Pezeron, F. Porteu, IEX-1: a new ERK substrate involved in both ERK survival activity and ERK activation, EMBO J. 21 (2002) 5151–5163.

[42] Y. Huang, C.D. Wright, C.L. Merkwan, N.L. Baye, Q. Liang, P.C. Simpson, T.D. O'Connell, An alpha1A-adrenergic-extracellular signal-regulated kinase survival signaling pathway in cardiac myocytes, Circulation 115 (2007) 763–772.

[43] A. Oganesian, V. Yarov-Yarovoy, W.C. Parks, D.A. Schwinn, Constitutive coupling of a naturally occurring human alpha1a-adrenergic receptor genetic variant to EGFR transactivation pathway, Proc. Natl. Acad. Sci. U. S. A. 108 (2011) 19796–19801.

[44] I.M. Kim, D.G. Tilley, J. Chen, N.C. Salazar, E.J. Whalen, J.D. Violin, H.A. Rockman, Beta-blockers alprenolol and carvedilol stimulate beta-arrestin-mediated EGFR transactivation, Proc. Natl. Acad. Sci. U. S. A. 105 (2008) 14555–14560.

[45] T. Noma, A. Lemaire, S.V. Naga Prasad, L. Barki-Harrington, D.G. Tilley, J. Chen, P. Le Corvoisier, J.D. Violin, H. Wei, R.J. Lefkowitz, H.A. Rockman, Beta-arrestin-mediated beta1-adrenergic receptor transactivation of the EGFR confers cardioprotection, J. Clin. Invest. 117 (2007) 2445–2458.

[46] Major cardiovascular events in hypertensive patients randomized to doxazosin vs chlorthalidone: the antihypertensive and lipid-lowering treatment to prevent heart attack trial (ALLHAT). ALLHAT Collaborative Research Group, JAMA 283 (2000) 1967–1975, (%19).

[47] J.N. Cohn, The Vasodilator-Heart Failure Trials (V-HeFT). Mechanistic data from the VA Cooperative Studies. Introduction, Circulation 87 (1993) VI1–VI4.

[48] M. Yang, F. Verfurth, R. Buscher, M.C. Michel, Is alpha1D-adrenoceptor protein detectable in rat tissues? Naunyn Schmiedebergs Arch. Pharmacol. 355 (1997) 438–446.

[49] K.P. Minneman, Heterodimerization and surface localization of G protein coupled receptors, Biochem. Pharmacol. 73 (2007) 1043–1050.